ISSN 0020-4412, Instruments and Experimental Techniques, 2024, Vol. 67, No. 5, pp. 902–910. © Pleiades Publishing, Ltd., 2024.

ELECTRONICS AND RADIO ENGINEERING

Quantum Noise Limited Nondegenerate Josephson Parametric Amplifier with Nb/Alox/Nb Junctions for Qubit Readout

I. S. Besedin[a], I. E. Pologov[a], L. V. Filippenko[b], V. P. Koshelets[b], and A. V. Karpov[a,*]

[a] *National University of Science and Technology MISIS, Laboratory of Superconducting Quantum Technologies, Moscow, 119049 Russia*

[b] *Kotelnikov Institute of Radio Engineering and Electronics, Russian Academy of Sciences, Moscow, 125009 Russia*

**e-mail: alexandre.karpov@yahoo.com*

Received November 27, 2023; revised May 30, 2024; accepted September 11, 2024

Abstract—Superconducting qubits have become a promising and rapidly growing research area over the last two decades. However, there are specific challenges when working with such a delicate system. One of them is the qubit state readout. Since a very small signal (of the order of 1 photon) is used for the readout, its detection is challenging and it requires low-noise cryogenic amplifiers working in the 3–12 GHz frequency range. Josephson parametric amplifiers (JPAs) are one of the most studied and developed candidates. Currently, several JPA designs offer low noise performance and instantaneous bandwidth from tens of MHz to several GHz; they are also becoming an integral part of circuit Quantum Electrodynamics (cQED) setups. In the current work, results are presented of the measurements of a JPA made of a coplanar waveguide with an array of three SQUIDs. Nondegenerate amplification and an amplifier added noise being close to the quantum limit are demonstrated.

DOI: 10.1134/S0020441224701495

1. INTRODUCTION

Reading the state of a quantum system is one of the most important stages of any work in the actively developing field of CQED (circuit quantum electrodynamics). Accurate reading is essential when observing quantum jumps [1], quantum trajectories [2, 3], implementation of quantum error correction [4], and observation of nonclassical states of light [5]. The power of the read signal in all these applications is very small (on the order of a few photons per band), and the signal must be amplified to be detected by the measurement equipment. As is known, any amplifier adds noise to the signal, and the issue of the amplifier's noise temperature becomes especially acute in the case of such weak signals.

The minimum possible added noise of an amplifier (the so-called quantum limit) is $T_Q = hf/2k_B$ [6], where h is Planck's constant, k_B is Boltzmann constant, and f is frequency of the amplified signal. At 8 GHz, the quantum limit of the amplifier's equivalent noise temperature is approximately 190 mK. Real amplifiers may be inferior to the ideal design for a number of reasons. For example, additional noise in an amplifier can be caused by thermal radiation from circuit elements, losses in the circuit, low quantum efficiency, shot noise, fluctuations, and carrier transport features in the sample.

A Josephson parametric amplifier (JPA) at a temperature of 10–50 mK and with an optimal circuit design can be free from all these additional noise sources; it allows amplification of microwave signals with minimal addition of noise, at the level of the quantum noise limit. However, one should take into account the noise level of the following amplification stage after the JPA in real measurements, where cryogenic transistor amplifiers are usually used. With a gain of the JPA equal to 10 dB and an equivalent noise temperature of the subsequent stage equal to 3 K, the contribution of the transistor amplifier to the chain noise can be 300 mK, i.e., be approximately equal to $1.5T_Q$ at 8 GHz, whereas the contribution will be 30 mK, i.e., small compared to T_Q, with a gain of the JPA of 20 dB.

In this paper, we present the results of the development of a niobium-based JPA consisting of a quarter-wave coplanar resonator with an array of three SQUIDs [7]. We demonstrate the presence of nondegenerate four-wave gain [8–12] and added noise close to the quantum limit. The creation of a JPA circuit based on niobium technology is of significant practical interest due to its durability and the higher critical temperature of the material compared to similar parameters of the widespread aluminum technology. The nondegenerate operating mode of the JPA is con-

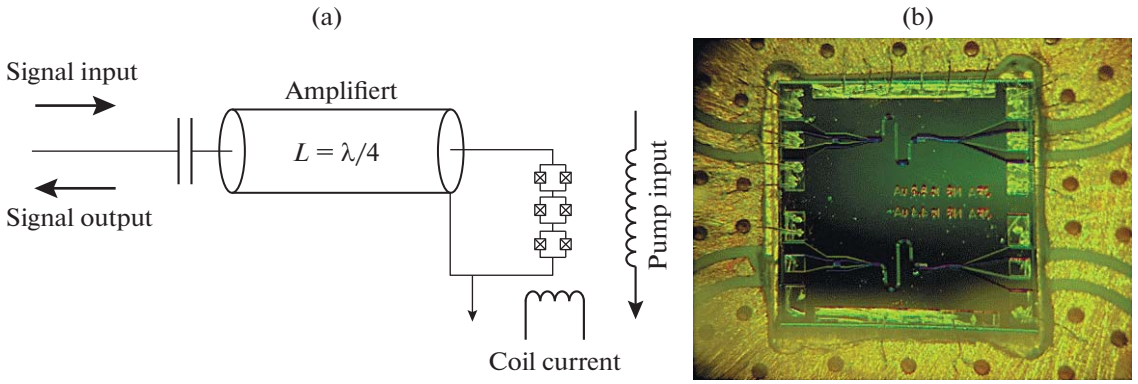

Fig. 1. Josephson contact amplifier sample design: **(a)** basic circuit diagram of the amplifier consists of a quarter-wave resonator and three SQUIDs, the signal and pump are supplied through two independent channels; **(b)** Photograph of a sample with two amplifier circuits in an experimental setup. Chip size 4 × 4 mm^2. Signal input is on the left, pump input is on the right.

venient for frequency separation of signal and pump channels.

2. DESCRIPTION OF THE SAMPLE AND MEASURING SETUP

The amplifier sample was fabricated using optical lithography in standard Nb/AlOx/Nb-in the process [13, 14]. The schematic diagram of the amplifier is shown in Fig. 1a. The amplified signal is fed to the amplifier input through a capacitive coupling element, then it enters a coplanar quarter-wave resonator loaded with an array of three DC SQUIDs. The inductance of Josephson contacts depends on the magnitude of the applied magnetic field on the SQUID. As a result, the operating frequency of the amplifier is retuned by an external magnetic field. Typically, the experiment records the current through the solenoid, which creates a magnetic field on the SQUID in the amplifier, and, as a result, the experimental data are presented as the dependence of the resonant frequency of the amplifier circuit on the current through the solenoid. The tuning range of the resonant frequency of the amplifier circuit coincides with the operating band of the amplifier. The critical current of the Josephson contacts was approximately 3.4 μA. The pump signal is supplied via a separate coplanar transmission line inductively coupled to the SQUIDs.

The amplifier housing is part of the test setup (Fig. 2). Depending on the size of the housing cavity above the sample, it is possible to excite a bulk mode that strongly interacts with the circuit of the device under test (e.g., [15]). We carried out initial tests (Fig. 3) in the holder described in [15], with a relatively high cavity resonant band (approximately 30 GHz), significantly exceeding the operating frequencies of the amplifier. To implement a nondegenerate amplifier, a housing with cavity dimensions providing resonance near 7.9 GHz was used. In this case, due to the volume resonance of the case, a two-circuit resonant circuit was obtained, which is necessary for the operation of a nondegenerate amplifier.

2. EXPERIMENTAL SETUP DIAGRAM AND MEASUREMENT RESULTS

The amplifier is placed in a cryostat and is maintained at a temperature of 34 mK. The pump signal and the signal from the network analyzer are fed to the pump input and signal input of the amplifier through cooled attenuators that prevent the passage of thermal noise. Josephson contacts are included in the SQUID circuit. The resonance in the cavity above the amplifier circuit is represented by a series circuit. The source of calibrated noise is matched loads located at physical temperatures of 34 mK and 3.5 K. For the convenience of the experiment, the “hot” load, the temperature of which is 3.5 K, is connected to the amplifier input through an attenuator cooled to 34 mK with an attenuation of 10 dB. The gain is measured by a network analyzer; the noise power at the amplifier output is measured by a spectrum analyzer.

3. AMPLIFIER FREQUENCY RETURN

The parametric amplifier is based on the effect of the dependence of the inductance of a SQUID included in a microwave resonator circuit on the external magnetic flux. The magnetic field passing through the SQUID has a constant and variable component. The constant component of the magnetic flux is created using a solenoid wound around the sample holder. The variable component of the magnetic flux is created using a microwave source connected to the pump port of the parametric amplifier circuit. Applying an external magnetic field to the solenoid reduces the resonant frequency of the resonator. The dependence of the resonant frequency on the applied field is

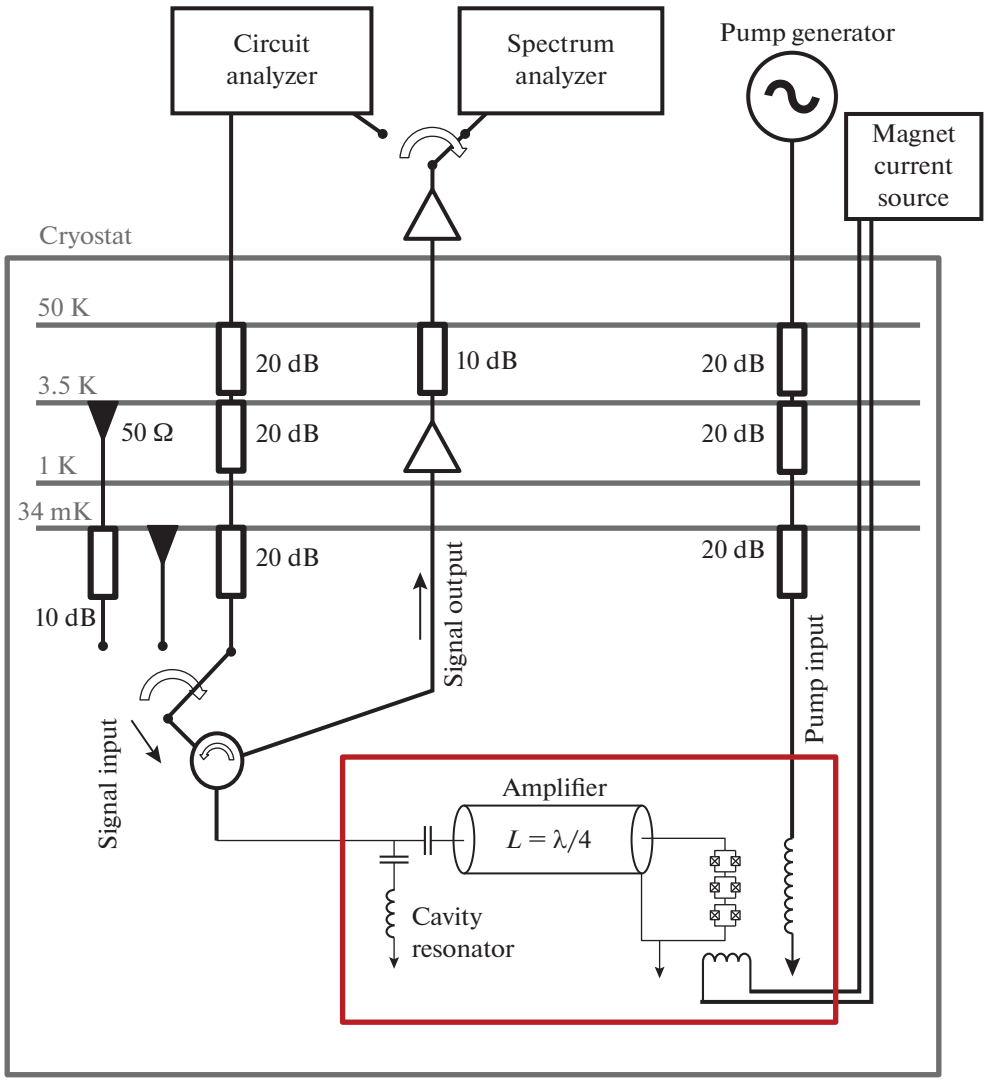

Fig. 2. Experimental setup for measuring the characteristics of a Josephson junction amplifier.

determined by measuring the reflection coefficient of microwave radiation from the signal input of a parametric amplifier with the pumping turned off.

The measured dependences of the resonant frequency of the amplifier on the current in the control solenoid are shown in Fig. 3. The data were obtained as a series of amplitude-frequency response (AFR) of the circuit, measured at different values of current in the solenoid. The width and intensity of the line on the AFR plane indicate the strength of the connection between the resonator in the amplifier circuit and the signal source. The studied sample has a tuning band from 7 to 9.2 GHz and can potentially amplify in this range; however, the blurring of the response to the AFR in the band 8.5–9.2 GHz may indicate a nonoptimal connection of the resonator with the signal source in this sub-range.

The calculated AFR of a parametric amplifier with resonance in the cavity of the housing (Fig. 4) is characterized by a splitting of the resonance near the natural resonance frequency of the housing and illustrates the possibility of implementing a two-circuit circuit of a nondegenerate amplifier. The color scale in Fig. 4a shows the level of reflection coefficient from the input to the amplifier circuit without pumping. The region of resonance splitting is highlighted by a dashed line (Fig. 4a). The calculation was carried out for the equivalent circuit in Fig. 2. The frequency dependence of the reflection coefficient from the circuit input for different values of the magnetic flux in the SQUIDs (Fig. 4b) in the highlighted region demonstrates the possibility of creating a two-circuit circuit, which is necessary for a nondegenerate amplifier. The corresponding experiments confirming the proposed model are presented below.

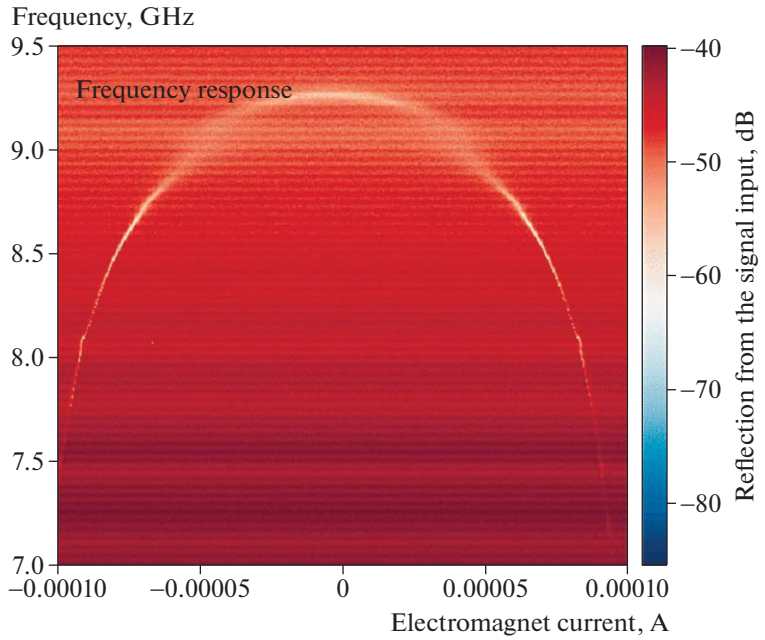

Fig. 3. Measured AFR of the parametric amplifier circuit depending on the applied external magnetic field (direct current in the solenoid). The resonant frequency of the amplifier appears as a feature in the plane of reflection coefficients.

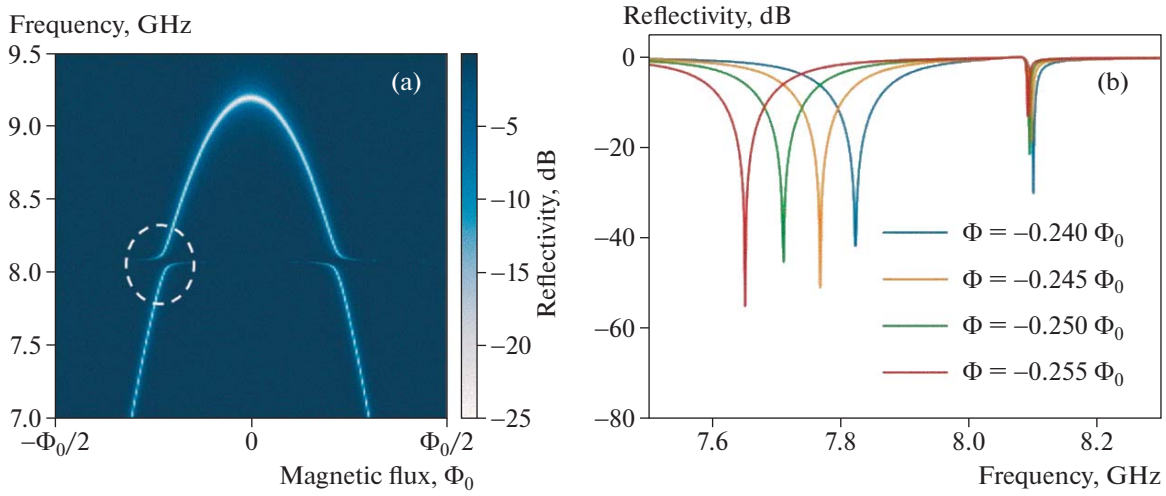

Fig. 4. (**a**) Calculated AFR of the input circuit of the parametric amplifier depending on the applied external magnetic field for a circuit with resonance in the housing cavity, as in the experiment in Fig. 2. The AFR region used to ensure the nondegenerate mode of the amplifier is highlighted by a dashed line (the corresponding experiment is shown in Fig. 6). (**b**) Calculated frequency response of the amplifier circuit for different values of magnetic flux in SQUIDs for the region marked by the dashed line in Fig. 4a.

4. OPTIMIZATION OF CONTROL PARAMETERS OF A PARAMETRIC AMPLIFIER

From the application point of view, to improve the accuracy of one-time qubit reading, it is important to optimize the control current, frequency, and power of the JPA. Measuring the accuracy of reading the state of a qubit is quite labor-intensive since it requires simultaneous control of both the qubit and the parametric amplifier. A similar value that characterizes the usefulness of an amplifier for such an application is the signal-to-noise ratio. In a linear approximation, this characteristic depends only on the signal frequency. The linear model is valid for low test signal power. The characteristic value of the power level below which the linear approximation is valid is the saturation power: the 1-dB compression point.

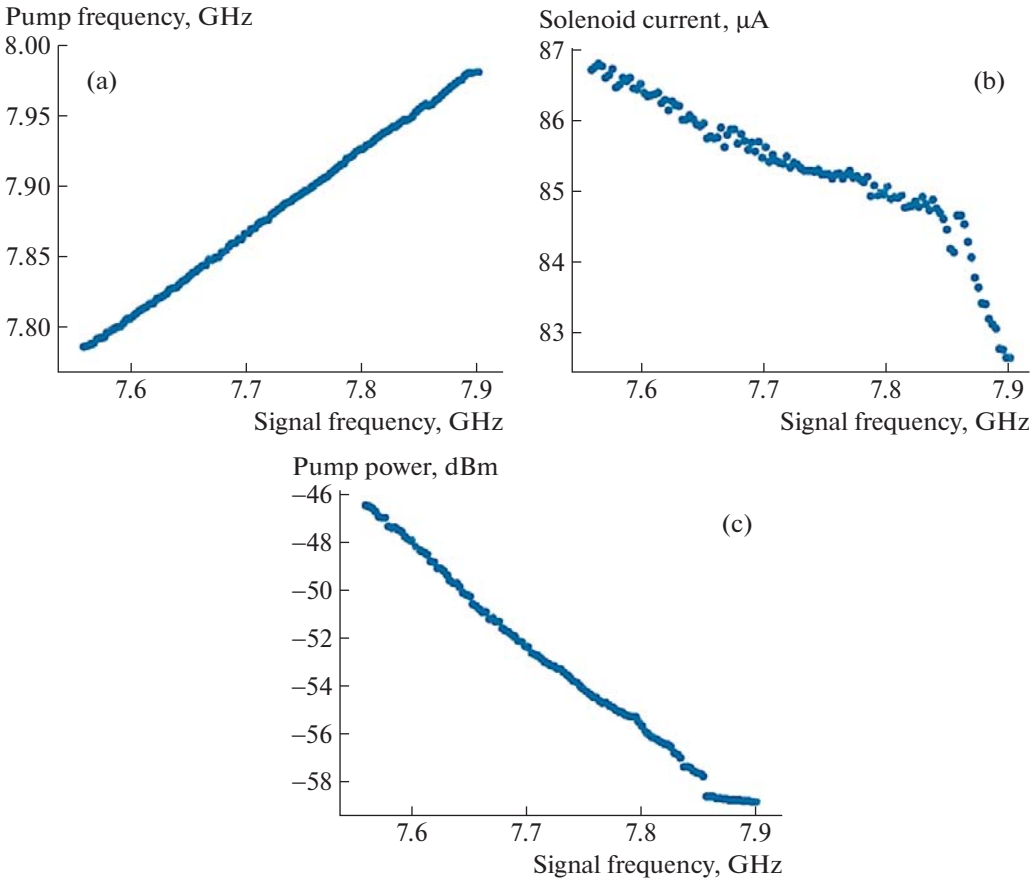

Fig. 5. Dependence of the optimal pumping and current parameters in the electromagnet on the target frequency (frequency of the amplified signal).

When using a parametric amplifier for single-shot dispersive readout of a qubit state, the bandwidth of the amplifier must be significantly larger than the bandwidth of the readout signal, which, in turn, is determined by the bandwidth of the readout resonator. Therefore, the optimization of the pump frequency and power, as well as the solenoid current, must be carried out for different frequencies of the test signal, the power of which corresponds to the power of the reading signal. In this experiment, optimization was performed in the frequency range of 7.4–8.2 GHz with a test signal power of –120 dBm. To determine the relative magnitude of the signal-to-noise ratio, multiple measurements of the transmission coefficient were performed using a vector network analyzer. The signal-to-noise ratio is proportional to the standard deviation of this quantity. The results of parameter optimization are shown in Fig. 5. As expected, for a nondegenerate amplifier, the pump frequency differs from the signal frequency by 150–200 MHz (Fig. 5a).

The measured frequency dependences of the JPA gain for each target optimization frequency are shown in Fig. 6. During the measurements, the optimal parameters of the mode from Fig. 5 were used. For each optimization frequency, two gain maxima are observed (in the signal band and in the mirror band), characteristic of a nondegenerate parametric amplifier. A gain of more than 15 dB is observed at the frequency selected for optimization (lower red bar) as well as at the mirror frequency (upper red bar). The pump frequency lies between the lower and upper gain bands (middle line). The difference between the pump frequency and the gain bands reaches 200 MHz, which is sufficient for frequency separation of the signal and pump channels.

5. MEASUREMENT OF GAIN AND EQUIVALENT NOISE TEMPERATURE

Measurements of the gain and noise temperature of the JPA were carried out using the method of reference noise signal sources. The reference noise source was a black body, namely two matched 50-ohm loads at known temperatures with known effective temperatures. The loads are connected one by one to the amplifier input, and the signal power at the output is measured using a spectrum analyzer. Reference loads emit a noise signal over a wide frequency range, including the mirror frequency. Therefore, it should

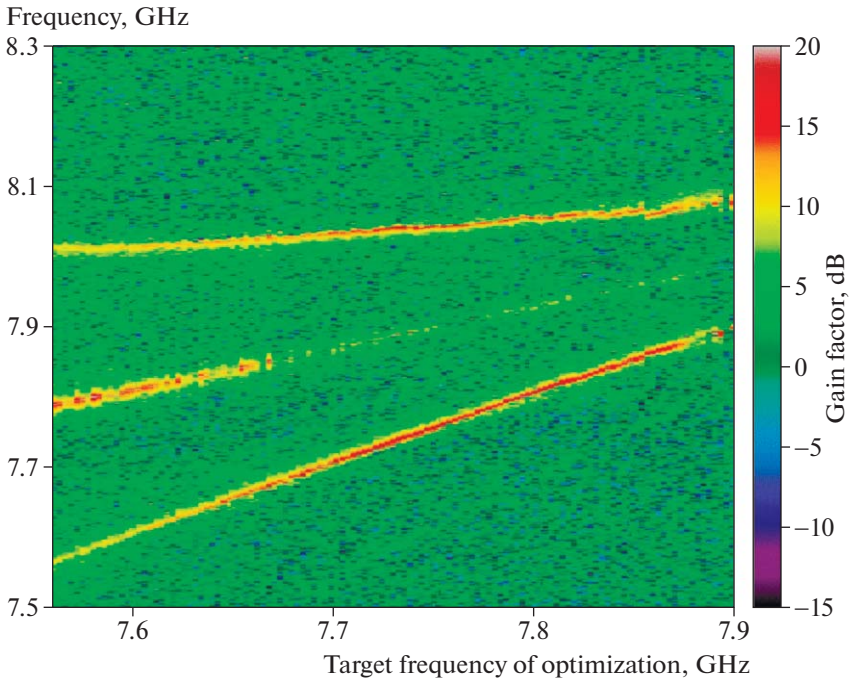

Fig. 6. Measured frequency dependences of the gain of the JPA for each target optimization frequency (with optimal mode parameters from Fig. 5). A gain of more than 15 dB is observed at the frequency selected for optimization (lower red bar) as well as at the mirror frequency (upper red bar). The pump frequency lies between the lower and upper gain bands (middle line). The difference between the pump frequency and the gain bands reaches 200 MHz.

be taken into account that the noise power at the output of the parametric amplifier comes through the signal and mirror channels. The power measured by the spectrum analyzer in frequency band B for a linear parametric amplifier is described by the formulas

$$P_{\text{out}}^1 = G_S B k_B \left(T_{\text{in}}^1 + T_n\right) + (G_I - 1) B k_B \left(T_{\text{in}}^1\right), \quad (1)$$

$$P_{\text{out}}^2 = G_S B k_B \left(T_{\text{in}}^2 + T_n\right) + (G_I - 1) B k_B \left(T_{\text{in}}^2\right), \quad (2)$$

where G_S and G_I are gain at the signal frequency and at the mirror frequency, T_{in}^1 and T_{in}^2 are equivalent noise temperatures of a black body (in Rayleigh–Jeans terms). Measured equivalent noise temperature of the amplifier T_n characterizes the signal channel. In the case when G_S and G_I are equal in magnitude and significantly exceed 1:

$$P_{\text{out}}^1 = G B k_B (2T_{\text{in}}^1 + T_n), \quad (3)$$

$$P_{\text{out}}^2 = G B k_B (2T_{\text{in}}^2 + T_n), \quad (4)$$

which gives the following equivalent noise temperature of the amplifier at the signal frequency:

$$T_n = \frac{2(T_{\text{in}}^1 - T_{\text{in}}^2)}{\frac{P_{\text{out}}^1}{P_{\text{out}}^2} - 1} - 2T_{\text{in}}^2, \quad (5)$$

Power P_{out}^1 and P_{out}^2 is measured at two different temperatures of the reference black body T_{in}^1 and T_{in}^2, connected to the input of the parametric amplifier. The solution of the system of two linear equations (3) and (4) for unknowns GT_n and G is sensitive to errors in values $T_{\text{in}}^1 - T_{\text{in}}^2$ and $T_{\text{in}}^1 P_{\text{out}}^2 - T_{\text{in}}^2 P_{\text{out}}^1$, so it is advisable to choose T_{in}^1 and T_{in}^2 in such a way that their difference and average are proportionate to T_n.

The advantage of the described method of measuring noise temperature and gain is the possibility of obtaining absolute values calibrated to the temperature of the reference load. The disadvantage of the method is the numerical instability of the system of equations with respect to power fluctuations and errors in the linear model. To calculate the noise power of the reference loads, the effective temperature T_{eff} of the loads was used, which corresponds to the noise power spectral density in Rayleigh–Jeans terms. The value of T_{eff} was calculated using the Cullen and Welton relationship [16]:

$$T_{\text{eff}} = \frac{hf}{2k_B} \coth\left(\frac{hf}{2k_B T}\right). \quad (6)$$

At 8 GHz, the effective cold load temperature T_{in}^2 was approximately 190 mK. The “hot” load, at a temperature of 3.5 K, is connected to the reference plane

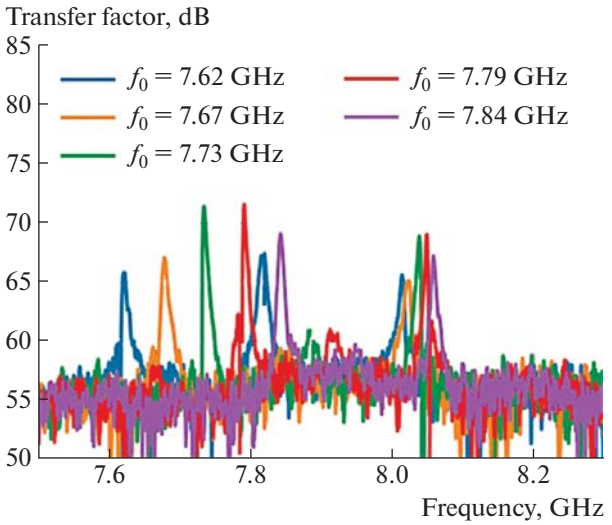

Fig. 7. Result of measuring the gain of a circuit consisting of a JPA and an amplifier on a transistor with high electron mobility. The gain is defined as the excess over the calibration curve; it reaches 15–17 dB. Target signal frequency for optimization is f_0.

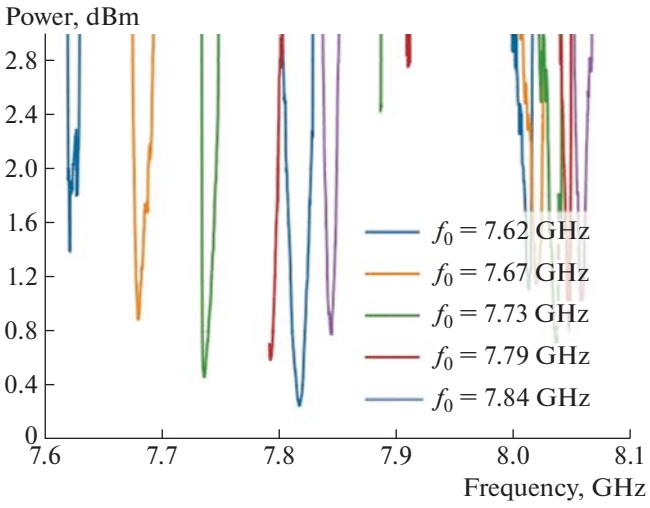

Fig. 8. Result of measuring the equivalent noise temperature of a circuit consisting of a JPA and an amplifier on a transistor with high electron mobility. Target signal frequency for optimization is f_0.

in front of the amplifier through an attenuator $L = 10$ dB, located at a temperature of 34 mK. The total noise power of the "hot" load was obtained by adding the radiation of the cold attenuator and the radiation of the load weakened by the attenuator:

$$T_{\text{in}}^{1} = \frac{T_{\text{eff Hot}}}{L} + T_{\text{eff Cold}}\left(1 - \frac{1}{L}\right). \quad (7)$$

At 8 GHz, the radiation temperature from the hot load was approximately $T_{\text{in}}^{1} = 350$ mK + 170 mK = 520 mK.

Another approach to measuring noise and gain is based on measuring the signal gain using a vector analyzer. This method does not require solving equations and gives quick results. The main disadvantage of this method is that the obtained gain and noise temperature values are not absolute but relative. In principle, by comparing the gain level with the result obtained by the two-matched load method at different temperatures, we can calibrate this result. The second method was used for quick diagnostics of the amplifier.

The results of measuring the gain and effective noise temperature of a circuit consisting of a parametric amplifier and a high electron mobility amplifier at the 3.5 K stage of a cryostat using the reference noise signal source method are shown in Figs. 7 and 8, respectively.

It is evident that the gain is nondegenerate [8, 10]: instead of one Lorentzian peak with a maximum at the pump frequency, two peaks are observed with maxima equidistant from the pump frequency. The split frequency response is the characteristic frequency response of a circuit consisting of two coupled resonators: in this case, a circuit composed of a cavity resonator in the amplifier case and a planar amplifier circuit. As a result, the resonance of the amplifier circuit is split into two, thereby changing the shape of the gain curve and the gain band [11, 12]. Nondegenerate amplification is extremely convenient when using the amplifier to measure superconducting qubits. Since the pumping is strongly detuned from the signal frequency, its influence on the system under study is excluded.

The frequency dependence of the gain coefficient obtained in the experiment (Fig. 7) is in good agreement with the calculated response for a two-circuit circuit of a nondegenerate amplifier (Fig. 4b). The frequencies with maximum gain in Fig. 7 correspond to the frequencies of the resonant peaks in Fig. 4b.

The measured gain reaches 15–17 dB, and the minimum noise of the amplification circuit approaches 0.4–0.5 K. Here the contribution of the transistor amplifier to the measured system noise is approximately 0.2–0.3 K, while the added noise of the JPA reaches 0.2 K and approaches the quantum limit for the operating frequency of 7.8 GHz.

6. SATURATION POWER

The amplifier saturation power was measured using a vector network analyzer. Absolute power values are obtained by combining the results of gain measurements by two methods. The point corresponding to saturation was chosen to be the compression point of 1 dB, i.e., the power at the input of the parametric amplifier circuit at which the gain is reduced by 1 dB compared to the gain in the low-power signal limit. The measurement results are shown in Fig. 9.

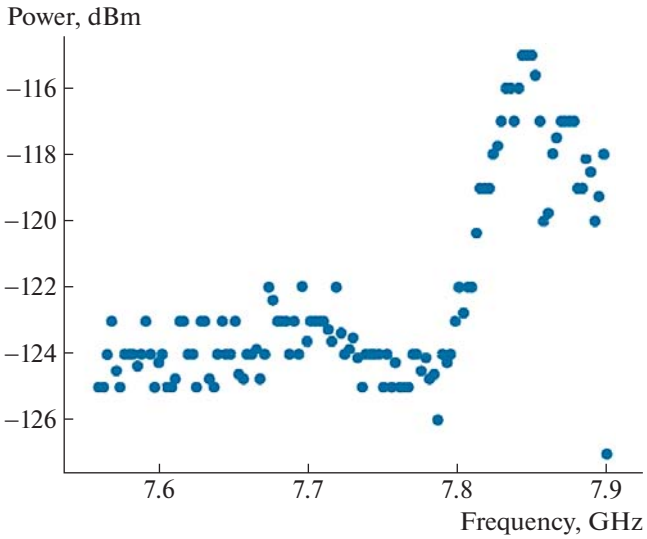

Fig. 9. Signal power level at 1-dB compression depending on the center frequency of the gain band of a tunable parametric amplifier.

The measured value of saturation power was −124 ± 2 dBm, which corresponds to approximately 10 photons of signal frequency with an accumulation time of 0.1 μs. The achieved values of saturation power allow the developed amplifier to be used to determine the quantum state of a qubit using the dispersion readout method.

7. CONCLUSIONS

This paper presents the characteristics of the developed parametric microwave amplifier consisting of a quarter-wave coplanar resonator with an array of three SQUIDs. The measured values of the equivalent noise temperature of the developed microwave amplifier on a Josephson contact are significantly lower in magnitude than the noise of a cryogenic amplifier on a transistor with high carrier mobility (2–3 K), which confirms the usefulness of the developed amplifier for constructing circuits for reading qubit states. The most reliable measurement of the absolute value of the equivalent noise temperature of an amplifier chain consisting of a JPA and a transistor amplifier is made using the reference noise source method. Two absolutely black bodies (absorbers) with an equivalent noise temperature of 190 and 520 mK were used as a reference signal source. The minimum measured noise temperature of the amplifier is close (within the measurement accuracy) to the quantum limit; it was 400–500 mK.

Nondegenerate mode of operation amplifier, typical for a circuit consisting of two coupled resonators, was demonstrated. Frequency separation of the gain and pump bands in a nondegenerate amplifier is convenient for isolating the readout qubit from the amplifier pump power. The measured saturation power level corresponds to a signal power of approximately 10 photons over an accumulation time of 0.1 μs, which is sufficient to handle typical signal powers when reading out qubit states.

FUNDING

The study was carried out with financial support from the Russian Science Foundation. (project no. 21-72-30026, https://rscf.ru/en/project/21-72-30026/). The production of experimental samples of the superconducting amplifier microcircuit was supported by a grant from the Russian Science Foundation (project no. 21-42-04421, https://rscf.ru/project/21-42-04421/).

CONFLICT OF INTEREST

The authors of this work declare that they have no conflicts of interest.

REFERENCES

1. Gambetta, J., Blais, A., Boissonneault, M., Houck, A.A., Schuster, D.I., and Girvin, S.M., *Phys. Rev. A,* 2008, vol. 77, p. 012112. https://doi.org/10.1103/PhysRevA.77.012112
2. Roch, N., Schwartz, M.E., Motzoi, F., et al., *Phys. Rev. Lett.,* 2014, vol. 112, p. 170501. https://doi.org/10.1103/PhysRevLett.112.170501
3. Weber, S.J., Murch, K.W., Kimchi-Schwartz, M.E., Roch, N., and Siddiqi, I., *Compt. Rend. Phys.,* 2016, vol. 17, p. 766. https://doi.org/10.1016/j.crhy.2016.07.007
4. Reed, M.D., Dicarlo, L., Nigg, S.E., Sun, L., Frunzio, L., Girvin, S.M., and Schoelkopf, R.J., *Nature,* 2012, vol. 482, p. 382. https://doi.org/10.1038/nature10786
5. Eichler, C., Bozyigit, D., Lang, C., Baur, M., Steffen, L., Fink, J.M., Filipp, S., and Wallraff, A., *Phys. Rev. Lett.,* 2011, vol. 107, p. 113601. https://doi.org/10.1103/PhysRevLett.107.113601
6. Clerk, A.A., Devoret, M.H., Girvin, S.M., Marquardt, F., and Schoelkopf, R.J., *Rev. Mod. Phys.,* 2010, vol. 82, p. 1155. https://doi.org/10.1103/RevModPhys.82.1155
7. Eichler, C. and Wallraff, A., *EPJ Quantum Technol.,* 2014, vol. 1, no. 2. https://doi.org/10.1140/epjqt2
8. Eichler, C., Salathe, Y., Mlynek, J., Schmidt, S., and Wallraff, A., *Phys. Rev. Lett.,* 2014, vol. 113, p. 110502. https://doi.org/10.1103/PhysRevLett.113.110502
9. Roy, A. and Devoret, M., *Compt. Rend. Phys.,* 2016, vol. 17, no. 7, p. 740. https://doi.org/10.1016/j.crhy.2016.07.012
10. Devoret, M. and Roy, A., *Compt. Rend. Phys.,* 2016, vol. 17, no. 7, p. 740. https://doi.org/10.1016/j.crhy.2016.07.012
11. Mutus, J.Y., White, T.C., Barends, R., et al., *Appl. Phys. Lett.,* 2014, vol. 104, p. 263513. https://doi.org/10.1063/1.4886408

12. Roy, T., Kundu, S., Chand, M., et al., *Appl. Phys. Lett.,* 2015, vol. 107, p. 262601. https://doi.org/10.1063/1.4939148

13. Dmitiriev, P.N., Ermakov, A.B., Kovalenko, A.G., et al., *IEEE Trans. Appl. Supercond.,* 1999, vol. 9, p. 3970. https://doi.org/10.1109/77.783897

14. Filippenko, L.V., Shitov, S.V., Dmitriev, P.N., et al., *IEEE Trans. Appl. Supercond.,* 2001, vol. 11, p. 816. https://doi.org/10.1109/77.919469

15. Averkin, A.S., Karpov, A., Shulga, K., Glushkov, E., Abramov, N., Huebner, U., Il'ichev, E., and Ustinov, A.V., *Rev. Sci. Instrum.,* 2014, vol. 85, p. 104702. https://doi.org/10.1063/1.4896830

16. Kerr, A.R., Feldman, M.J., and Pan, S.-K., NRAO electronics division internal report no. 304 (also distributed as MMA Memo № 161), 1996. https://www.gb.nrao.edu/electronics/edir/edir304.pdf.

SPELL; OK